



Comprehensive bioanalytical multi-imaging by planar chromatography in situ combined with biological and biochemical assays highlights bioactive fatty acids in abelmosk

N.G.A.S. Sumudu Chandana, Gertrud E. Morlock*

Justus Liebig University Giessen, Institute of Nutritional Science, Chair of Food Science, and TransMIT Center for Effect-Directed Analysis, Heinrich-Buff-Ring 26-32, 35392 Giessen, Germany

ARTICLE INFO

Keywords:

Antibacterial
Enzyme inhibitor
Radical scavenger
Bioprofiling
Planar bioassay
HPTLC-UV/Vis/FLD-EDA-HESI-HRMS

ABSTRACT

The identification of the bioactivity of individual compounds in natural products is helpful to understand their therapeutic applications. Thus, a bioanalytical multi-imaging screening was developed and applied to 54 bark, leaf and seed extracts of Sri Lankan *Abelmoschus moschatus* (abelmosk) to find out the most bioactive individual compounds. The focus was laid on a comprehensive bioactivity profiling of its extracts. High-performance thin-layer chromatography (HPTLC) was hyphenated with seven effect-directed assays (EDA), i. e. biological (Gram-negative *Aliivibrio fischeri* and Gram-positive *Bacillus subtilis*), biochemical (α -glucosidase, β -glucosidase, acetylcholinesterase and tyrosinase) and chemical (2,2-diphenyl-1-picrylhydrazyl) assays. This multi-imaging was complemented by ultraviolet (UV), white light (Vis), fluorescence detection (FLD) and eight microchemical derivatizations. Heated electrospray ionization high-resolution mass spectrometry (HESI-HRMS) was used to characterize the most prominent multi-potent compound zone. It consisted of coeluting unsaturated fatty acids (linoleic acid and oleic acid), but also saturated fatty acids (palmitic acid and to a lower extent stearic acid, arachidic acid and behenic acid). For confirmation of the detected effects (antibacterial, free radical scavenger and inhibitor of α -glucosidase, β -glucosidase, acetylcholinesterase and tyrosinase), oleic acid was exemplarily analyzed by co-development and overlapped application (with sample). The proven effects underlined the beneficial health effects derived from unsaturated fatty acids like oleic acid. Exemplarily, the α -glucosidase and tyrosinase inhibition responses of the multi-potent compound zone were quantified equivalently in reference to oleic acid. The comparable results obtained by two independent enzymatic responses successfully proved the use of biochemical quantification by planar enzyme assays, and thus the new method based on HPTLC-UV/Vis/FLD-EDA-HESI-HRMS.

1. Introduction

Ongoing attention is paid to medicinal plants for the discovery of safe drugs for humans [1], as market expectations for drugs produced by synthetic drug libraries have not been fulfilled [2]. Around 21,000 plant species are possibly used as medicinal plants, whereof the majority is inexpensive, readily available and low in side effects [3]. This huge potential offered by nature needs to be exploited. Latest innovative extraction methods using natural deep eutectic solvents [4] or natural products rich in bioactive compounds or biofortified extracts [5,6] attract interest in the cosmetic, medicinal, nutritional and industrial fields. Plant-derived drugs account for 33% of the total drug production

in the industry [7]. In consequence, proof-based strategies for their quality control and unequivocal identification are demanded [8]. In particular, such strategies are treasured which include the evaluation of the bioactivity profile of products containing so-called active ingredients.

Abelmoschus moschatus (abelmosk, Malvaceae) is used in traditional medicine treatments and was selected for the intended bioprofiling as a plant-derived drug. Pharmacological effects are reported especially for its kidney-shaped seeds in a green-brownish capsule [9] and its lobed leaves [10]. It grows annually as a shrub or small tree and grows in tropical Asia, Africa and South America. Antiaging, antidiabetic, anti-oxidative, anticonvulsant, antidepressant, antimicrobial,

* Corresponding author.

E-mail address: Gertrud.Morlock@uni-giessen.de (G.E. Morlock).

antiproliferative, anxiolytic, antilithiatic, diuretic, hepatoprotective, hemagglutinating, hypnotic, memory strengthening and muscle relaxant activities have been reported for it [11].

Seven effect-directed assays were selected for the bioprofiling. The detection of new plant-derived antibiotics against Gram-positive/-negative bacteria is demanded due to the worldwide antibiotic resistance caused by improper use and misuse of antibiotics [12,13]. The detection of antidiabetic effects is also important, as the diabetes mellitus type 2 patients are predicted to be 592 million by 2035 [14]. Most synthetic drugs target one pathway to control hyperglycemia [15], whereas plant-derived glucosidase inhibitors result in a reduced post-prandial blood glucose level by its influence on carbohydrate digestion [16] with only few or less side effects compared to synthetic drugs [17–19]. On another enzymatic pathway, tyrosinase is responsible for melanogenesis in the skin of mammals [20], and plant-derived tyrosinase inhibitors are treasured ingredients in natural cosmetics [21]. In the same way, polyphenol oxidases are responsible for browning reactions of fungi, fruits, vegetables etc. [22]. The Alzheimer disease is a lethal neurodegenerative disorder predicted to be 150 million by 2050 [23]. Its current pharmacotherapy is most dependent on N-methyl D-aspartate antagonists and cholinesterase inhibitors [24,25]. For the latter, there is interest in inhibitors from natural sources with only minor side effects [26]. For an appropriate physiological function, a balance between free radicals or reactive oxygen/nitrogen species (generated as by-products in metabolic processes) and antioxidants is essential to limit degenerative diseases [27]. In particular, the detection and use of plant-derived radical scavengers or antioxidants is attractive [28].

Hence, multi-imaging bioanalytical screening methods are demanded to discover new bioactive compounds in natural sources. Hyphenated high-performance thin-layer chromatography (HPTLC) stands for minimalistic sample preparation but maximalistic detection performance to collect comprehensive information [29–31]. All in all, 18 different detection modes were used, i.e. ultraviolet (UV), white light (Vis), fluorescence detection (FLD), eight microchemical derivatizations and seven effect-directed assays (EDA). As samples, bark, leaf and seed of Sri Lankan abelmosk were screened to point to the most pronounced antibacterial, antidiabetic, anti-tyrosinase, anti-acetylcholinesterase and radical scavenging compounds, of which the most effective zone was characterized by heated electrospray ionization high-resolution mass spectrometry (HESI-HRMS).

2. Experimental

2.1. Chemicals and materials

HPTLC plates silica gel 60 with and without F₂₅₄, also respective HPTLC plates MS-grade, all 20 × 10 cm, *Bacillus subtilis* spores (BGA, DSM 618 strain) and ascorbic acid (99%) were obtained from Merck, Darmstadt, Germany. *Aliivibrio fischeri* bacteria (NRRI-B11177, strain 7151) were purchased from Leibniz Institute, DSMZ, German Collection of Microorganisms and Cells Cultures, Berlin, Germany. Acetic acid (100%), 2-aminoethoxydiphenyl borate (98%), hydrochloric acid (≥37%), kojic acid (98%), 3-(4,5-dimethylthiazol-2-yl)-2,5-diphenyltetrazolium bromide (MTT, 98%), polyethylene glycol (PEG) 8000, tris (hydroxymethyl) aminomethane (Tris, 99.8%), sulphuric acid (≥96%) and vanillin (≥99%) were purchased from Carl Roth, Karlsruhe, Germany. Acetone (100%), ethyl acetate (≥99.8%), n-hexane (≥95%) and orthophosphoric acid (≥85%) were bought from Th. Geyer, Renningen, Germany. Acarbose, AChE lyophylisate (6.66 U/mL, from *Electrophorus electricus* with ≥245 U/mg, 10 kU/vial), p-aminobenzoic acid (≥99%), p-anisaldehyde (98%), aniline (99.5%), 3-cyclohexyl amino-propane sulfonic acid (CAPS, ≥98%), 2,2-diphenyl-1-picrylhydrazyl (DPPH[•], 95%), α-glucosidase (10 U/mL, from *Saccharomyces cerevisiae* with 1000 U/vial), imidazole (≥99.5%), ninhydrin, primuline, physostigmine, sodium acetate (≥99%), tyrosinase (400 U/mL, from mushroom with ≥1000 U/mg), oleic, linoleic and palmitic acids (all ≥99%) were

purchased from Sigma-Aldrich, Steinheim, Germany. 2-Naphthyl-β-D-glucopyranoside (95%) and β-glucosidase (1000 U/mL, from almond with 3040 U/mg) were purchased from abcr, Karlsruhe, Germany. α-Naphthyl acetate (≥99%) was bought from AppliChem, Darmstadt, Germany. Ethanol (≥99.8%) was purchased from Fisher Scientific, Loughborough, UK. 2-Naphthyl-α-D-glucopyranoside was bought from Flurochem, Hadfield, UK. Toluene (≥99.7%) was purchased from LGC standard, Wesel, Germany. Fast Blue B salt (~95%) was purchased from MP Biomedical, Illkirch, France. (2S)-2-Amino-3-(3,4-dihydroxy phenyl)propanoic acid (levodopa) was obtained from Santa Cruz Biotechnology, Dallas, TX, USA. Methanol (ca. 100%) was purchased from VWR International, Darmstadt, Germany. Bidistilled water was prepared by a Destamat Bi 18E (Heraeus, Hanau, Germany). The polypropylene box (26.5 cm × 16 cm × 10 cm) was from KIS, ABM, Wolframs-Eschenbach, Germany.

2.2. Sample origin, preparation and standard solutions

Sri Lankan *Abelmoschus moschatus* IDs 1–6 were from Karapitiya and IDs 7–18 from Wanduramba, both suburbs of Galle. The collected bark pieces, leaves and seeds were cleaned and shade-dried (4–5 days, 30 °C, 65% RH). Each sample was ground at 15,000 rpm for 6 min (Tube Mill, IKA, Staufen, Germany), 500-μm sieved (stainless steel test sieve, VWR International) and stored protected in the dark at ca. 18 °C. Seed and leaf powder (200 mg each) were extracted with 2 mL ethanol – water 4:1 (100 mg/mL) in a conical Eppendorf tube (15 mL, polypropylene), whereas 3 mL was used for extraction of 200 mg bark powder (67 mg/mL). For quantification, seed extract was 1:4 diluted with ethanol – water 4:1 (25 mg/mL). All suspensions were placed in an ultrasonic bath (480 W, frequency 35 kHz, Sonorex Digi plus DL 255H, Bandelin, Berlin, Germany) at 25 °C for 30 min and centrifuged (Heraeus Labofuge 400, Thermo Scientific, Dreieich, Germany) at 2400×g for 10 min. Each supernatant was transferred to a sampler vial, stored at ca. 8 °C in the dark. Methanolic solutions of oleic acid (1.35, 0.675 and 0.25 mg/mL), palmitic acid and linolic acid (each 0.25 mg/mL) were used.

2.3. HPTLC method

The extracts were applied as 8-mm band on the HPTLC plate silica gel F₂₅₄ at a 150-nL/s dosage speed (Automatic TLC Sampler ATS 4, CAMAG, Muttenz, Switzerland) and dried in a stream of cold air for 2 min. The distance from the left plate edge or bottom edge was 10 mm and the track distance ≥9.4 mm. If required the plate was cut (TLC SmartCut, CAMAG). The plate was developed with toluene – ethyl acetate – methanol 6:5:2 or toluene – ethyl acetate 7:3 up to 65 mm in the twin trough chamber (20 × 10 cm, biostep or CAMAG) and dried (2 min). Each chromatogram was documented at UV 254 nm, FLD 366 nm and white light illumination (TLC Visualizer, CAMAG). Operation was controlled by visionCATS software version 2.5.18262.1 (CAMAG).

2.4. Chemical profiling

Eight identical chromatograms with representative extracts were detected via the following detection modes: (A) UV 254 nm, (B) Vis, (C) FLD 366 nm as well as after derivatization (immersion speed 3 cm/s, immersion time 2 s, TLC Immersion Device III, CAMAG) with (D) primuline reagent (250 mg primuline, 50 mL water, 200 mL acetone) at UV 366 nm after 1- min drying, (E) p-anisaldehyde sulphuric acid reagent (1.5 mL methoxybenzaldehyde, 210 mL methanol, 25 mL acetic acid, 13 mL sulphuric acid), (F) vanillin sulphuric acid reagent (3 g vanillin, 247 mL ethanol, 3 mL sulphuric acid), (G) p-aminobenzoic acid reagent (2 g 4-aminobenzoic acid, 50 mL glacial acetic acid, 50 mL water, 2 mL orthophosphoric acid), (H) the latter at FLD 366 nm, (I) diphenylamine aniline orthophosphoric acid reagent (100 mL diphenylamine and aniline, each 2% in isopropanol, 20 mL orthophosphoric acid), (J) ninhydrin reagent (500 mg ninhydrin, 230 mL ethanol, 20 mL glacial acetic

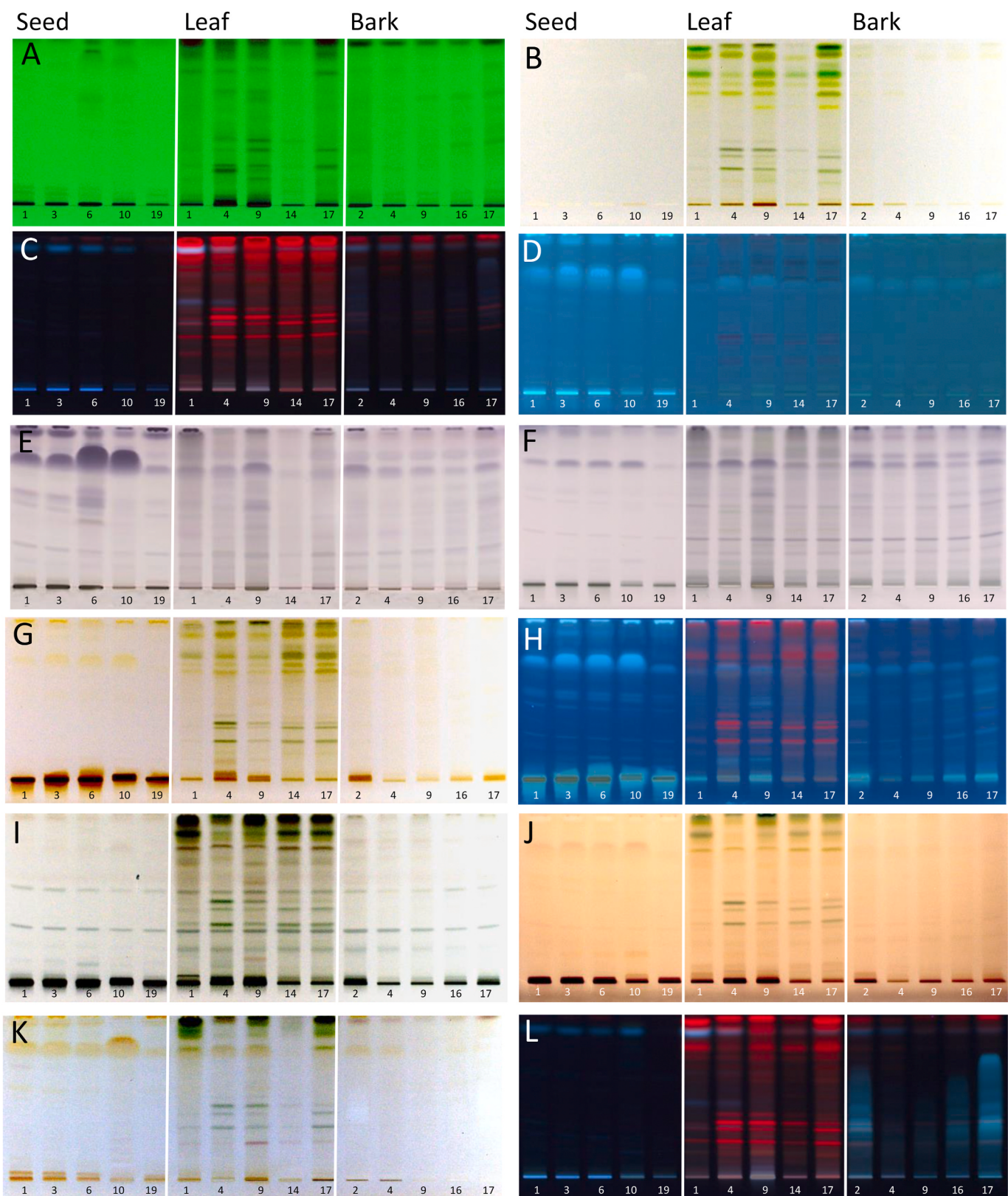


Fig. 1. Chemical profiling: HPTLC chromatograms of selected bark (1340 µg/band each), leaf and seed extracts (1000 µg/band each) of abelmosk (respective IDs per track) on HPTLC plates silica gel 60 F₂₅₄ with toluene – ethyl acetate – methanol 6:5:2, detected at (A) UV 254 nm, (B) white light illumination, (C) FLD 366 nm, and by (D) primuline reagent at FLD 366 nm, (E) p-anisaldehyde sulphuric acid reagent, (F) vanillin sulphuric acid reagent, (G) p-aminobenzoic acid reagent, (H) same at FLD 366 nm, (I) diphenylamine aniline orthophosphoric acid reagent, (J) ninhydrin reagent, (K) Fast Blue B salt reagent and (L) natural product reagent at FLD 366 nm; E-G and I-K documented at white light illumination. (For interpretation of the references to color in this figure legend, the reader is referred to the Web version of this article.)

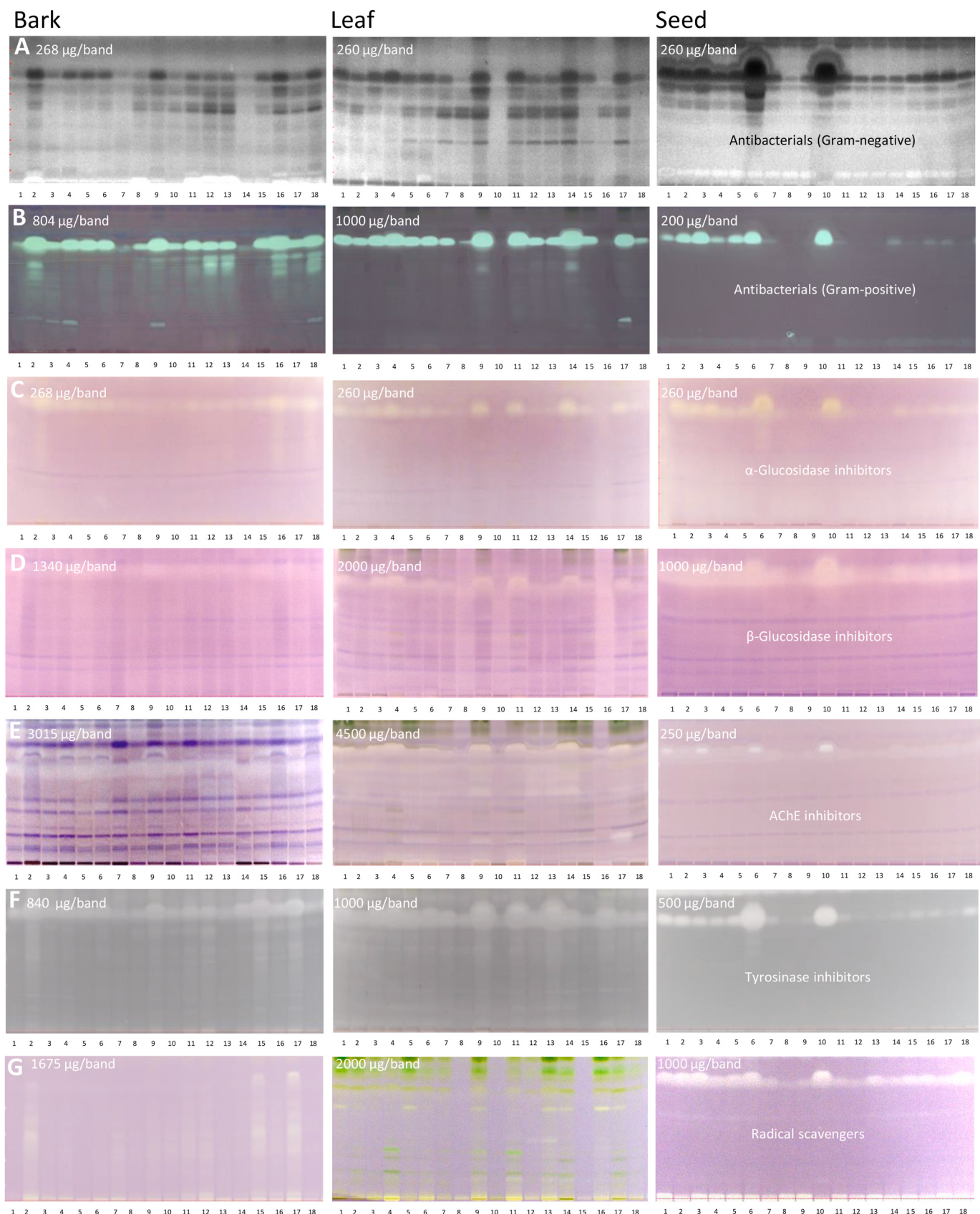


Fig. 2. Effect-directed profiling: HPTLC (bio)autograms of bark, leaf and seed extracts of abelmosk (IDs 1–18 applied depending on assay response and separated as in Fig. 1) detected by (A) Gram-negative *Alivibrio fischeri* (grey-scale image of bioluminescence) and (B) Gram-positive *Bacillus subtilis* bioassays as well as (C) α-glucosidase, (D) β-glucosidase, (E) AChE and (F) tyrosinase inhibition assays, and (G) DPPH[•] assay; (B–G) detected at white light illumination.

acid), (K) Fast Blue B salt reagent (250 mg Fast Blue B salt, 250 mL ethanol 70%), (E-K) Vis detection after heating at 140 °C for max. 5 min (TLC Plate Heater, CAMAG), and (L) natural product reagent (1.5 g 2-aminoethoxydiphenyl borate, 250 mL ethanol) at FLD 366 nm after air-drying.

2.5. Effect-directed profiling

HPTLC plates were pre-washed using methanol – water 3:1, V/V, dried at 110 °C for 30 min and stored protected until use. Extract volumes were applied depending on the assay response (see Fig. 2). After development, respective positive controls (PC) were applied as edge track pattern or above the solvent front. HPTLC chromatograms were further dried for 15 min (Automatic Developing Chamber ADC 2, CAMAG) to remove all residual mobile phase traces and then immersed in the respective assay solution/suspension (TLC Immersion Device III) or piezoelectrically sprayed with these (Derivatizer, both CAMAG). The plate was horizontally incubated in a moistened polypropylene box, afterward dried and documented at Vis (reflectance mode, TLC Visualizer, CAMAG), if not stated otherwise.

2.5.1. Gram-negative *Aliivibrio fischeri* bioassay

According to Ref. [32], the bacterial culture (prepared as in DIN EN ISO 11348-1) was piezoelectrically sprayed onto the chromatogram (4 mL, blue nozzle, level 6). The instant bioluminescence was recorded over a 30 min period (time interval 3 min, exposure time 60 s, Bioluminizer, CAMAG). The PC was caffeine (1–7 µL/band, 0.5 mg/mL in methanol).

2.5.2. Gram-positive *Bacillus subtilis* bioassay

According to Ref. [33], the chromatogram was dipped in the bacterial suspension (immersion speed 3.5 cm/s, immersion time 5 s) and incubated at 37 °C for 2 h. The plate was dipped into a 0.2% PBS-buffered MTT solution (immersion speed 3.5 cm/s, immersion time 1 s) and heated at 50 °C for 5 min. The PC was tetracycline (1–7 µL/band, 0.004 mg/mL in ethanol).

2.5.3. α -Glucosidase inhibition assay

According to Ref. [33], the chromatogram was piezoelectrically sprayed (2 mL, yellow nozzle, level 6) with substrate solution (12 mg 2-naphthyl- α -D-glucopyranoside in a mixture of 9 mL ethanol and 1 mL 10 mM sodium chloride) and dried (2 min). For pre-wetting, 1 mL sodium acetate buffer (10.25 g sodium acetate in 250 mL water adjusted to pH 7.5 with acetic acid 0.1 M) was piezoelectrically sprayed using the same nozzle, followed by 2 mL α -glucosidase (10 U/mL in sodium acetate buffer, pH 7.5). After plate incubation at 37 °C for 15 min, 0.75 mL Fast Blue B salt solution (4 mg/mL in water) was piezoelectrically sprayed and the plate was dried (2 min). The PC was acarbose (1–18 µL/band, 3 mg/mL in ethanol). Absorbance measurement at 546 nm was performed using the mercury lamp and an inverse scan, as zones were brighter than the background. Quantification was performed via peak area.

2.5.4. β -Glucosidase inhibition assay

The β -glucosidase inhibition assay was performed analogously to the α -glucosidase inhibition assay, but β -glucosidase (3040 U/mL) and 2-naphthyl- β -D-glucopyranoside were used. Incubation took longer (30 min). The PC was imidazole (1–7 µL/band, 1 mg/mL in ethanol).

2.5.5. AChE inhibition assay

According to Ref. [32], the chromatogram was piezoelectrically sprayed (green nozzle, level 6) with 1 mL Tris-HCl buffer (pH 7.8), then 3 mL AChE solution (6.66 U/mL in Tris-HCl buffer plus 1 mg BSA) and incubated at 37 °C for 25 min. The substrate solution (0.75 mL, ethanolic α -naphthyl acetate solution and aqueous Fast Blue B salt solution, 1:2) was piezoelectrically sprayed (red nozzle, level 6) and the plate was

dried (2 min). The PC was physostigmine (2–8 µL/band, 2 µg/mL in ethanol).

2.5.6. Tyrosinase inhibition assay

According to Ref. [34], the chromatogram was piezoelectrically sprayed (blue nozzle, level 6) with 2 mL substrate solution (45 mg levodopa, 25 mg CAPS and 75 mg PEG 8000 dissolved in 10 mL 0.02 M phosphate buffer, pH 6.8), after drying (2 min) with 2 mL tyrosinase solution (400 U/mL phosphate buffer), incubated at ca. 20 °C for 15 min and dried (8 min). The PC was kojic acid (1–6 µL/band, 0.1 mg/mL in ethanol). Absorbance measurement at 579 nm was performed as mentioned in 2.5.3.

2.5.7. Radical-scavenging assay

According to Ref. [35], the chromatogram was immersed into 0.02% methanolic DPPH[•] solution (immersion speed 2 cm/s, immersion time 2 s), followed by air-drying for 90 s and at 60 °C for 30 s (TLC Plate Heater). The PC was ascorbic acid (2–7 µL/band, 0.1 mg/mL in water).

2.6. HESI-HRMS

Samples were applied in duplicate on MS-grade HPTLC plates and cut into two halves after development. One plate half was subjected to the tyrosinase inhibition assay to transfer the coordinates/positions of the bioactive zones in the autogram to the other plate half (marked by a soft pencil). The marked zones were eluted with methanol (60 s, flow rate 0.1 mL/min) using an elution head-based interface (Plate Express, Advion, Ithaca, NY, USA) coupled to HESI-Q Exactive Plus mass spectrometer (Thermo Fisher Scientific, Dreieich, Germany). Full scan HPTLC-HESI-HRMS spectra (*m/z* 50–750) were recorded in the positive and negative ionization mode with a spray voltage of ±3.5 kV, the capillary temperature of 270 °C, sheath gas of 20 (arbitrary units), aux gas of 10 (arbitrary units) and S-Lens RF level of 50. The obtained spectra were processed with Xcalibur 3.0.63 software (Thermo Fisher Scientific). The plate background was subtracted from each analyte spectrum.

3. Results and discussion

3.1. Development of the HPTLC method

Bark pieces, leaves and seeds of *Abelmoschus moschatus* samples (Figure S1, IDs 1–6 collected from Karapitiya and IDs 7–18 from Wanduramba, both suburbs of Galle, Sri Lanka) were collected from 18 scrubs, cleaned, shade-dried, ground and sieved to obtain a homogenous powder. For the fiber-rich bark, a higher extraction volume was used. Three extraction solvent mixtures of different polarity (methanol – water, ethanol – water and *n*-hexane – ethyl acetate, all 4:1, V/V) were investigated for their extraction efficiency of the bioactive compounds from the different abelmosk parts (Figure S2). Among these, the mixture of ethanol and water 4:1 (medium polarity) extracted all bioactive compounds, including those found in the more polar/apolar extracts, as proven by the *Aliivibrio fischeri* bioassay. This bioassay is recommended as a start assay, since it detects the highest number of bioactive compounds based on our experience. For separation on normal phase HPTLC silica gel plates, four different solvent combinations were studied as mobile phase. Toluene – ethyl acetate – methanol 6:5:2 (V/V/V) or the more apolar toluene – ethyl acetate 7:3 (V/V) were suited for subsequent analyses, as the bioactive compound zones were sufficiently sharp and spread along the migration distance after the *Aliivibrio fischeri* bioassay (Figures S3 and S4). Both developments up to 65 mm took about 20 min.

3.2. Chemical profiling

Five representative extracts (each of bark, leaf and seed) were analyzed by the new method. Their UV/Vis/FLD images (Fig. 1 A-C)

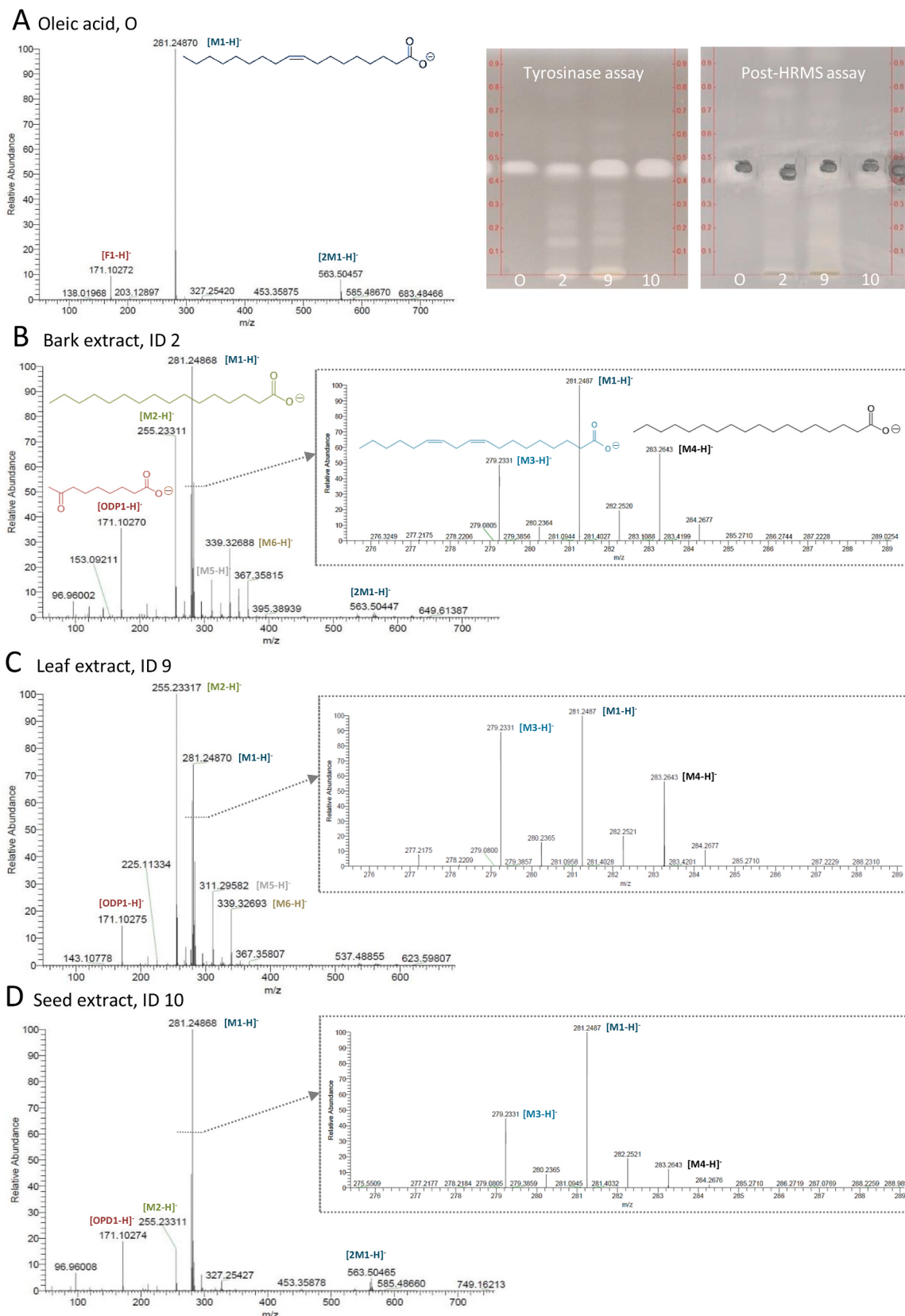


Fig. 3. HPTLC-HESI⁻-HRMS spectra of the multi-potent compound zone in abelmosk bark (ID 2; 800 ng/band), leaf (ID 9; 1000 ng/band) and seed extracts (ID 10; 500 ng/band) as well as oleic acid (1.3 µg/band, hR_F 45) applied in duplicate on respective MS-grade HPTLC plates, developed with toluene – ethyl acetate 7:3, for zone marking, one plate part detected at Vis after the tyrosinase inhibition assay and the other after HRMS recording (post-HRMS assay), showing oleic acid at m/z 281.2487 and palmitic acid at m/z 255.2331 as most intense mass signals, but also linoleic acid at m/z 279.2331 and stearic acid at m/z 283.2643 (all assignments in Table 1).

revealed most detectable compounds to be present in the leaf extracts. These contained greenish chlorophylls in the Vis chromatogram, prominent as red fluorescent and UV-absorbing bands in the FLD and UV chromatograms, respectively. Since not all components in an extract are detectable by UV/Vis/FLD or MS, eight derivatization reagents were exploited to widen the detectable compound range. The information on functional groups is also helpful for later characterization of selected bioactive compounds and identification of their chemical nature. Eight identical chromatograms were detected via twelve different detection modes (Fig. 1). A lipophilic compound zone was detected at hR_F 75 by the primuline reagent at FLD in all extracts, but in particular in the seed extracts (Fig. 1 D). Using the *p*-anisaldehyde sulphuric acid reagent, additional organic compounds were detected at Vis. The previously detected lipophilic compound zone at hR_F 75 was also detected by this reagent, although the horizontal pattern across all tracks was differently pronounced (detecting another coeluting compound for IDs 6 and 10). However, many other compounds were observed by this more universal derivatization reagent, which have not been detected before (as not UV/Vis/FLD active or lipophilic, Fig. 1 E). The similarly detecting vanillin sulphuric acid reagent showed comparatively less and differently intense compounds in the profile (Fig. 1 F). Saccharides were selectively detected at Vis by the *p*-aminobenzoic acid reagent (Fig. 1 G/H, also detects acids and the lipophilic compound at hR_F 75) and diphenylamine aniline orthophosphoric acid reagent (Fig. 1 I). For the given mobile phase system, all saccharides remained at the start zone. In all extracts, two greenish glycosides at hR_F 30 and hR_F 57 were newly detected at Vis after the diphenylamine aniline orthophosphoric acid reagent, also weakly blue fluorescent at FLD after the *p*-aminobenzoic acid reagent (Fig. 1 H). The respective yellow zones were not or hardly detectable via the comparatively less sensitive Vis detection (Fig. 1 G). Via the ninhydrin reagent, primary (or secondary) amino group-containing compounds were detected at Vis in the start zones, whereas no additional compound zone was observed along the developing distance (Fig. 1 J). As for the saccharides, the amino acids remained at the start for the given mobile phase. Via the Fast Blue B salt reagent only the previous compound zone at hR_F 75 was detected at Vis in the seed extracts, and two further at the start zone (Fig. 1 K versus 1 B). Using the natural product reagent at FLD, blue fluorescent flavonoid-like compounds were revealed in bark extract IDs 2, 16 and 17 (Fig. 1 L; an acid addition to the mobile phase would be needed to sharpen the tailing zones).

3.3. Effect-directed profiling

In order to obtain information on bioactive compounds, all extracts were subjected to effect-directed assays, including two antibacterial assays (against Gram-negative *Aliivibrio fischeri* and Gram-positive *Bacillus subtilis*), four enzymatic assays (against α - and β -glucosidase, AChE and tyrosinase) and a chemical radical scavenging assay (DPPH $^\bullet$). *Aliivibrio fischeri* is a marine bacterium that emits brilliant greenish-blue light above a certain cell density ($>10^9/\text{mL}$) for quorum sensing. In the *Aliivibrio fischeri* bioassay, antibacterial compounds were detected as dark or bright zones due to their impact on the energetic metabolism related to the bioluminescence of the *Aliivibrio fischeri* bacteria. In the bioautograms of the three plant parts, several antibacterial compounds were detected as dark zones reducing the bioluminescence on the otherwise bioluminescent plate background (depicted as greyscale image, Fig. 2 A). Among these, the previously detected zone at hR_F 75 revealed an antibacterial effect in almost all extracts. In particular, in seed extract IDs 1–6 and 10, this compound zone showed a strong antibacterial response against the Gram-negative bacteria (evident at a glance, as almost the same amount was applied for the different plant parts). Also, the opposite probiotic effect was detected in the bark and seed extracts, *i.e.* compounds at the start zone (bark) and at hR_F 10 (seed) which enhanced the bacterial bioluminescence. All bioactive zones increased in intensity in the bioautograms monitored over 30 min,

which proved the pronounced antibacterial effect. For the Gram-positive *Bacillus subtilis* bioassay, the bark and leaf volumes were increased by a factor of 3–4. Colorless bright zones indicated antibacterials on an MTT-violet plate background (colored by living bacteria). Again, an intense antibacterial zone was discovered at hR_F 75 in all three extract types (Fig. 2 B). Similar to the previous antibacterial pattern (not evident at a glance, as higher volumes applied for bark/leaf), again seed extract IDs 1–6 and 10 displayed a strong antibacterial effect. The strong similar responses in both orthogonal bacterial assays suggest that antibacterial compounds are tentatively produced at a higher amount in the seeds of Karapitiya (IDs 1–6) than Wanduramba (IDs 7–18). Our results are in accordance to a previous study, in which a moderate antimicrobial activity was reported against two Gram-positive (*Staphylococcus aureus* and *Bacillus cereus*) and three Gram-negative bacteria (*Escherichia coli*, *Shigella dysenteriae* and *Shigella sonnei*) for ethanolic extracts of leaf, bark, seed and fruit pulp [36].

In the following enzyme inhibiting assays, inhibitors were detected as colorless bright zones on a violet or grey plate background. The horizontal α -/ β -glucosidase inhibition patterns across all samples were in accordance with the previous antibacterial patterns. Thus, the previous antibacterial zone at hR_F 75 showed also α -/ β -glucosidase inhibitory effects (Fig. 2 C/D), and it was concluded to be the same bioactive (multi-potent) compound. However, its inhibition was much stronger against α -glucosidase than β -glucosidase (4–5 times higher volumes applied). The same multi-potent compound zone at hR_F 75 showed AChE and tyrosinase inhibition, especially in the mentioned seed extract IDs 1–6 and 10 (Fig. 2 E/F). Diverse much weaker AChE/tyrosinase inhibitors appeared for highly increased volumes applied for bark and leaf extracts (11/3 and 17/4 fold for AChE/tyrosinase, respectively *versus* Fig. 2 A). Another weaker tyrosinase inhibitor in the seed extracts was observed near the solvent front. Radical (DPPH $^\bullet$) scavengers appeared as bright zones at the start zone (indicating polar compounds) on a violet plate background. In particular in the seed extracts, the multi-potent zone at hR_F 75 was proven to be also a radical scavenger (Fig. 2 G).

A cross-check over the 54 abelmosk extracts and seven assays (Fig. 2) showed that the bioactivity profiles of the three different plant parts had comparatively more activity patterns in common than different. The seed extract IDs 1–6 and 10 were more potent than other seeds, bark and leaf. The multi-potent compound at hR_F 75 was most prominently detected in the seven assays, highlighting especially antibacterial, anti- α -glucosidase and anti-tyrosinase activities. The anti- β -glucosidase, anti-AChE and radical scavenging activities were comparatively weaker. Effective compounds also remained at the start zone, and further studies with acidic polar mobile phases are of interest.

3.4. HPTLC-HESI-HRMS of the multi-potent compound zone

The lipophilic multi-potent compound zone at hR_F 75 (Figs. 1 and 2) was assumed to be a fatty acid, and oleic acid was chosen as representative. The latter and selected samples were applied twice on a plate and developed with a mobile phase reduced in elution power (now hR_F 45, Figure S4 D?). One cut plate section was subjected to the tyrosinase assay to mark the bioactive zones on the other section, on which the assay was performed as proof of proper positioning after the HRMS recording of the eluted zones (post-HRMS assay, Fig. 3). In the positive ionization mode, the recorded HPTLC-HESI-HRMS spectra of the respective bioactive zone in the bark, leaf and seed extracts showed two oxidized degradation products (ODPs) of fatty acids. These mass signals were tentatively assigned to be the sodium adducts of 8-oxo-nonanoic acid at m/z 195.0991 [$\text{ODP1}+\text{Na}]^+$ (base peak) and of dihydroxydecanoic acid at m/z 227.1252 [$\text{ODP2}+\text{Na}]^+$ (Figure S5). In the negative ionization mode, the recorded mass spectra showed several distinct mass signals, and even further ones when zooming in the base peak range (Fig. 3). The spectra proved that the mass signals obtained from each multi-potent zone of the three extract types matched to the deprotonated molecules of oleic acid C18:1 at m/z 281.2487 [$\text{M1}-\text{H}]^-$,

Table 1

Assignment of the HPTLC-HESI-HRMS signals obtained from oleic acid used as reference and the respective multi-potent compound zone at hR_F 45 in three *Abelmoschus moschatus* extracts.

ID	Observed m/z	Theoretical m/z	Formula	Mass error (ppm)	Tentative assignment	
HPTLC-HESI⁻-HRMS						
Reference	281.24870	281.24860	$C_{18}H_{33}O_2^-$	-0.60	Oleic acid	[M1-H] ⁻
Bark ID 2	339.32687	339.32685	$C_{22}H_{43}O_2^-$	-0.06	Behenic acid	[M6-H] ⁻
	311.29568	311.29555	$C_{20}H_{39}O_2^-$	-0.42	Arachidic acid	[M5-H] ⁻
	283.26430	283.26425	$C_{18}H_{35}O_2^-$	-0.18	Stearic acid	[M4-H] ⁻
	281.24868	281.24860	$C_{18}H_{33}O_2^-$	-0.28	Oleic acid	[M1-H] ⁻
	279.23309	279.23295	$C_{18}H_{31}O_2^-$	-0.63	Linoleic acid	[M3-H] ⁻
	255.23311	255.23295	$C_{16}H_{32}O_2^-$	-0.63	Palmitic acid	[M2-H] ⁻
Leaf ID 9	339.32705	339.32685	$C_{22}H_{43}O_2^-$	-0.59	Behenic acid	[M6-H] ⁻
	311.29568	311.29555	$C_{20}H_{39}O_2^-$	-0.42	Arachidic acid	[M5-H] ⁻
	283.26436	283.26425	$C_{18}H_{35}O_2^-$	-0.39	Stearic acid	[M4-H] ⁻
	281.24870	281.24860	$C_{18}H_{33}O_2^-$	-0.75	Oleic acid	[M1-H] ⁻
	279.23312	279.23295	$C_{18}H_{31}O_2^-$	-0.75	Linoleic acid	[M3-H] ⁻
	255.23317	255.23295	$C_{16}H_{32}O_2^-$	-0.98	Palmitic acid	[M2-H] ⁻
Seed ID 10	283.26427	283.26425	$C_{18}H_{35}O_2^-$	-0.07	Stearic acid	[M4-H] ⁻
	281.24868	281.24860	$C_{18}H_{33}O_2^-$	-0.28	Oleic acid	[M1-H] ⁻
	279.23312	279.23295	$C_{18}H_{31}O_2^-$	-0.61	Linoleic acid	[M3-H] ⁻
	255.23317	255.23295	$C_{16}H_{32}O_2^-$	-0.86	Palmitic acid	[M2-H] ⁻
Oxidized degradation product (ODP)	171.10271	171.10266	$C_9H_{15}O_3^-$	-0.29	8-Oxo-nonanoic acid	[ODP1-H] ⁻
HPTLC-HESI⁺-HRMS						
	195.09918	195.09917	$C_9H_{16}O_3Na^+$	-0.05	8-Oxo-nonanoic acid	[ODP1+Na] ⁺
	227.12523	227.12538	$C_{10}H_{20}O_4Na^+$	0.66	Dihydroxydecanoic acid	[ODP2+Na] ⁺

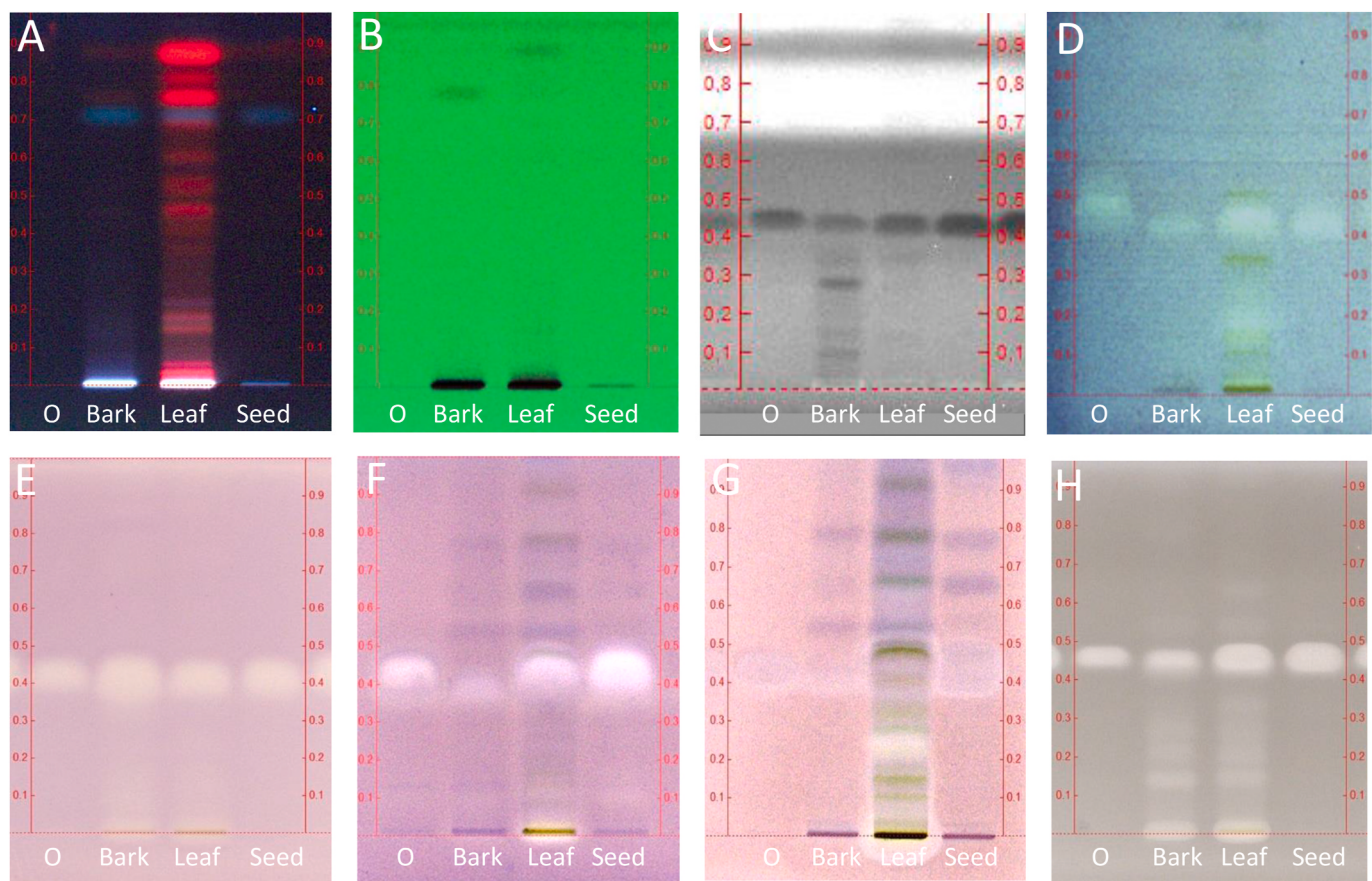


Fig. 4. Confirmation of the multi-potent compound assignment by co-development with exemplarily oleic acid (O, 1.3 μ g/band), detected at (A) FLD 366 nm, (B) UV 254 nm, after (C) Gram-negative *Aliivibrio fischeri* bioassay (grey-scale image of bioluminescence), as well as at Vis after (D) Gram-positive *Bacillus subtilis* bioassay and (E) α -glucosidase, (F) β -glucosidase, (G) AChE and (H) tyrosinase inhibition assays; chromatographic system as in Fig. 3.

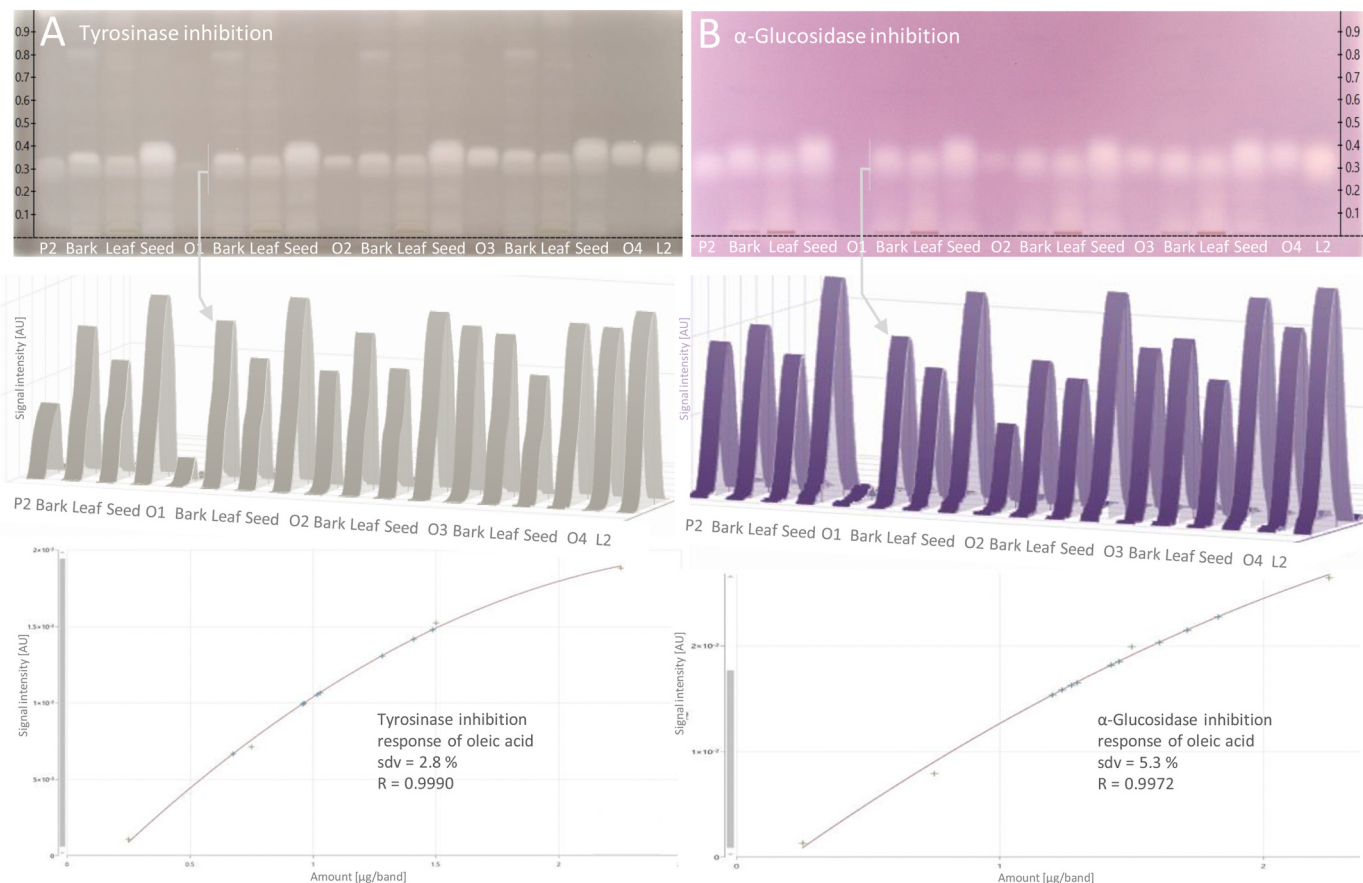


Fig. 5. Enzymatic quantification for equivalency calculation of the detected (A) tyrosinase and (B) α -glucosidase inhibiting compound zone: Autograms of abelmosk ID 6 extracts of bark (8 μ L, 540 μ g/band), leaf (2 μ L, 200 μ g/band) and seed (diluted 1:4, 1 μ L, 25 μ g/band) applied 4-fold along with palmitic acid (P2), linoleic acid (L2) as well as oleic acid calibration levels (O1–O4; 0.25 mg/mL, 1, 3, 6 and 9 μ L, 0.25–2.25 μ g/band); chromatographic system as in Fig. 3; respective densitograms at 546 nm and 579 nm (inverse absorbance measurement) as well as calibration curve plots.

palmitic acid C16:0 at m/z 255.2329 [M2-H] $^-$, linoleic acid C18:2 at m/z 279.2329 [M3-H] $^-$ and stearic acid C18:0 at m/z 283.2642 [M4-H] $^-$ (Table 1). Further, arachidic acid C20:0 at m/z 311.2955 [M5-H] $^-$ and behenic acid C22:0 at m/z 339.3268 [M6-H] $^-$ were detected in leaf and bark extracts. The oxidized fatty acid degradation product 8-oxo-nona-noic acid [37] was confirmed as deprotonated molecule at m/z 171.1027 [ODP1-H] $^-$. In agreement with our results, abelmosk seed was reported to be rich in unsaturated fatty acids and to contain about 40% linoleic acid, 30% oleic acid, 20% palmitic acid and 4% stearic acid as main fatty acid composition [38]. For bark and leaf, fatty acid values were not available. It is known that unsaturated linoleic acid and also oleic acid can easily be oxidized and that the fatty acid profile can vary naturally (e.g., less polyunsaturated fatty acids are formed at a warmer location than colder). This and also the different extraction methods

explain why the fatty acid distribution including degradation products may differ to our results.

3.5. Confirmation of the assignment

The tentatively assigned multi-potent compound zone to be coeluting fatty acids was confirmed by overlapped application with oleic acid as reference. Thus, the oleic acid migrated partly also within the abelmosk matrix (Figure S6). As a result, the oleic acid and the multi-potent compound were detected as common band, which confirmed the assignment by HPTLC-HESI-HRMS and multi-imaging. A sample comparison confirmed that fatty acids were more abundant in abelmosk seed than leaf and bark (Figure S7). Further the multi-potent activity of oleic acid was successfully proven in all assays (Fig. 4).

Table 2

Enzymatic quantification for equivalency calculation of the multi-potent compound zone in three different abelmosk extracts as well as response ratios for palmitic acid (P2) and linoleic acid (L2), all in reference to oleic acid (O2, all standard level 2) via the HPTLC-tyrosinase assay-Vis and HPTLC- α -glucosidase assay-Vis (as in Fig. 5).

Abelmosk extract ID 6	HPTLC-tyrosinase assay		HPTLC- α -glucosidase assay	
	Content of oleic acid (%)	Precision (%RSD, n = 4)	Content of oleic acid (%)	Precision (%RSD, n = 4)
Bark, 540 μ g/band	0.3	5.7	0.3	8.8
Leaf, 200 μ g/band	0.6	3.7	0.6	3.0
Seed, 25 μ g/band	10.2	2.9	10.8	2.7
Mean		4.1	Mean	4.8
Factor seed/bark	34		36	
Factor seed/leaf	17		18	
Peak area O2	0.0071	Response ratio to O2	0.0079	Response ratio to O2
Peak area P2	0.0066		0.0185	
Peak area L2	0.0249		0.0384	

3.6. Enzymatic quantifications for equivalency calculation

The comparison of results obtained by different methods is important for method verification. Hence, two different assays were evaluated concerning their calibration performance and quantitative results (Fig. 5). For this comparison, factors of influence and systematic errors were limited using the same extracts, standard dilution, application volumes, working range, automated application and piezoelectric spraying device. The coefficient of correlation of the polynomial calibration curve of oleic acid was 0.9990 (sdv 2.8%) and 0.9972 (sdv 5.3%) for the tyrosinase and α -glucosidase inhibition response, respectively. The respective mean precision ($n = 4$) of the oleic acid analysis in three different abelmosk extract types was 4.1% and 4.8% for the tyrosinase and α -glucosidase inhibition (Table 2). The bioactivity response of each abelmosk extract was calculated equivalently to the bioactivity response of oleic acid. It was 0.3%, 0.6% and 10.2% for bark, leaf and seed extracts, respectively, for the tyrosinase inhibition and almost the same (0.3%, 0.6% and 10.8%) for the α -glucosidase inhibition. The high activity of exemplarily seed extract ID 6 (Fig. 2) was confirmed. The seed had a 34 or 36-fold higher inhibiting activity (against tyrosinase or α -glucosidase, respectively) than the respective bark, and was 17 or 18-fold higher than the leaf. The comparison of the bioactivity responses of the three fatty acids (at the same amount) revealed that individual fatty acids contribute differently in its activity to the overall effect (Table 2). This has to be studied in detail in the future and highlights that individually active fatty acid responses and its meaning are still not explored to the full.

4. Conclusions

Comprehensive information was obtained by HPTLC-UV/Vis/FLD-EDA-HESI-HRMS on bioactive compounds present in 54 bark, leaf and seed extracts of abelmosk. In particular, antibacterial as well as α -glucosidase and tyrosinase inhibition effects were evident. In most extracts, a multi-potent compound zone was prominently detected by seven assays. It was identified to be coeluting fatty acids by HPTLC-HESI-HRMS, multi-imaging and co-chromatography (even in the matrix by overlapped application). All assay responses were successfully proven for oleic acid as reference, and this bioanalytical screening highlighted the bioactivity potential of unsaturated fatty acids. The multi-imaging (via all in all 19 detection modes) provided comprehensive information about multi-potent compounds and sample diversity. Such information is considered elementary for the assurance of the product quality in the field of botanicals, foods and medicinal plants, which are the backbone of traditional medicine.

CRediT author statement

N.G.A.S. Sumudu Chandana: Investigation, Writing - original draft preparation
Gertrud E. Morlock: Supervision, Writing - original draft preparation, Writing- Reviewing and Editing

Declaration of competing interest

The authors declare that they have no known competing financial interests or personal relationships that could have appeared to influence the work reported in this paper.

Acknowledgment

Thank is owed to the Food Science group for their technical guidance during this project and Merck, Darmstadt, Germany, for the supply of plates. Instrumentation was partially funded by the Deutsche Forschungsgemeinschaft (DFG, German Research Foundation) – INST 162/471-1 FUGG; INST 162/536-1 FUGG.

Appendix A. Supplementary data

Supplementary data to this article can be found online at <https://doi.org/10.1016/j.talanta.2020.121701>.

Supplementary data

Supplementary data can be found at ...

References

- [1] S. Gayibova, E. Ivanisová, J. Árvay, M. Hřstková, M. Slávik, J. Petrová, L. Hleba, T. Tóth, M. Kacániová, T. Ariov, In vitro screening of antioxidant and antimicrobial activities of medicinal plants growing in Slovakia, *J. Microbiol. Biotechnol. Food Sci.* 8 (2019) 1281–1289.
- [2] A.G. Atanasov, B. Waltenberger, E.-M. Pferschy-Wenzig, T. Linder, C. Wawrosch, P. Uhlir, V. Temml, L. Wang, S. Schwaiger, E.H. Heiss, J.M. Rollinger, D. Schuster, J.M. Breuss, V. Bochkov, M.D. Mihovilovic, B. Kopp, R. Bauer, V.M. Dirsch, H. Stuppner, Discovery and resupply of pharmacologically active plant-derived natural products: a review, *Biotechnol. Adv.* 33 (2015) 1582–1614.
- [3] B.N. Tefera, Y.-D. Kim, Ethnobotanical study of medicinal plants in the Hawassa Zuria district, Sidama zone, Southern Ethiopia, *J. Ethnobiol. Ethnomed.* 15 (2019) 25.
- [4] X. Liu, S. Ahlgren, H.A.A.J. Korthout, L.F. Salomé-Abarca, L.M. Bayona, R. Verpoorte, Y.H. Choi, Broad range chemical profiling of natural deep eutectic solvent extracts using a high performance thin layer chromatography-based method, *J. Chromatogr. A* 1532 (2018) 198–207.
- [5] V. Bardot, A. Escalon, I. Ripoche, S. Denis, M. Alric, S. Chalancor, P. Chalard, C. Cotte, L. Berthomier, M. Leremboure, M. Dubourdeaux, Benefits of the ipowder® extraction process applied to *Melissa officinalis* L.: improvement of antioxidant activity and in vitro gastro-intestinal release profile of rosmarinic acid, *Food & Function* 11 (2020) 722–729.
- [6] Morlock, G.E., Heil, J., Bardot, V., Lenoir, L., Cotte, C., Dubourdeaux, M., Assessment of botanicals fortified by the addition of concentrated plant infusions via planar chromatography hyphenated to effect directed assays and high-resolution mass spectrometry, *Food Chem.*, (in submission).
- [7] M.J. Cheesman, A. Ilanko, B. Blonk, I.E. Cock, Developing new antimicrobial therapies: are synergistic combinations of plant extracts/compounds with conventional antibiotics the solution? *Pharmacogn. Rev.* 11 (2017) 57–72.
- [8] M. Jamshidi-Aidji, G.E. Morlock, From bioprofiling and characterization to bioquantification of natural antibiotics by direct bioautography linked to high-resolution mass spectrometry: exemplarily shown for *Salvia miltiorrhiza* root, *Anal. Chem.* 88 (2016) 10979–10986.
- [9] H.S. Sheik, N. Vedaiyan, S. Singaravel, Evaluation of *Abelmoschus moschatus* seed extract in psychiatric and neurological disorders, *Int. J. Basic Clin. Pharmacol.* 3 (2014) 845–853.
- [10] S. Babitha, H.G.A. Deepu, T. Nageena, Antimotility and antisecretory related anti diarrhoeal activity of the *Abelmoschus moschatus* medik in experimental animal models, *International Journal of Pharmacy and Pharmaceutical Sciences* 10 (2018) 108–111.
- [11] A.T. Pawar, N.S. Vyawahare, Antiurolithiatic activity of *Abelmoschus moschatus* seed extracts against zinc disc implantation-induced urolithiasis in rats, *J. Basic Clin. Pharm.* 7 (2016) 32–38.
- [12] P.D. Gupta, T.J. Birdi, Development of botanicals to combat antibiotic resistance, *J. Ayurveda Integr. Med.* 8 (2017) 266–275.
- [13] M.U. Anyanwu, R.C. Okoye, Antimicrobial activity of Nigerian medicinal plants, *Journal of Intercultural Ethnopharmacology* 6 (2017) 240–259.
- [14] L. Guariguata, D.R. Whiting, I. Hambleton, J. Beagley, U. Linnenkamp, J.E. Shaw, Global estimates of diabetes prevalence for 2013 and projections for 2035, *Diabetes Res. Clin. Pract.* 103 (2014) 137–149.
- [15] H.S. El-Abhar, M.F. Schaalan, Phytotherapy in diabetes: review on potential mechanistic perspectives, *World J. Diabetes* 5 (2014) 176–197.
- [16] Y. Sivasothy, K.Y. Loo, K.H. Leong, M. Litaudon, K. Awang, A potent alpha-glucosidase inhibitor from *Myristica cinnamomea* King, *Phytochemistry* 122 (2016) 265–269.
- [17] L. Flores-Bocanegra, M. González-Andrade, R. Bye, E. Linares, R. Mata, α -Glucosidase inhibitors from *Salvia cincinata*, *J. Nat. Prod.* 80 (2017) 1584–1593.
- [18] S.M. Fayaz, V.S. Suvanish Kumar, K.G. Rajanikant, Finding needles in a haystack: application of network analysis and target enrichment studies for the identification of potential anti-diabetic phytochemicals, *PloS One* 9 (2014), e112911.
- [19] J. William, P. John, M.W. Mumtaz, A.R. Ch, A. Adnan, H. Mukhtar, S. Sharif, S. A. Raza, M.T. Akhtar, Antioxidant activity, α -glucosidase inhibition and phytochemical profiling of *Hyophorbe lagenicaulis* leaf extracts, *PeerJ* 7 (2019), e7022.
- [20] S. Zolghadri, A. Bahrami, M.T. Hassan Khan, J. Munoz-Munoz, F. Garcia-Molina, F. Garcia-Canovas, A.A. Saboury, A comprehensive review on tyrosinase inhibitors, *J. Enzyme Inhib. Med. Chem.* 34 (2019) 279–309.
- [21] S.Y. Lee, N. Baek, T.-G. Nam, Natural, semisynthetic and synthetic tyrosinase inhibitors, *J. Enzyme Inhib. Med. Chem.* 31 (2016) 1–13.
- [22] P. Garcia, I.A. Ramallo, R.L.E. Furlan, Reverse phase compatible TLC-bioautography for detection of tyrosinase inhibitors, *Phytochem. Anal.* 28 (2017) 101–105.

- [23] J. Korabecny, M. Andrs, E. Nepovimova, R. Dolezal, K. Babkova, A. Horova, D. Malinak, E. Mezeiova, L. Gorecki, V. Sepsova, M. Hrabinova, O. Soukup, D. Jun, K. Kuca, 7-Methoxytacrine-*p*-Anisidine hybrids as novel dual binding site acetylcholinesterase inhibitors for Alzheimer's disease treatment, *Molecules* 20 (2015) 22084–22101.
- [24] H. Kim, Detection of severity in Alzheimer's disease (AD) using computational modeling, *Bioinformation* 14 (2018) 259–264.
- [25] M. Kozurkova, S. Hamulakova, Z. Gazova, H. Paulikova, P. Kristian, Neuroactive multifunctional tacrine congeners with cholinesterase, anti-amyloid aggregation and neuroprotective properties, *Pharmaceuticals* 4 (2011) 382–418.
- [26] A. Gholamhoseinian, M.N. Moradi, F. Sharifi-far, Screening the methanol extracts of some Iranian plants for acetylcholinesterase inhibitory activity, *Research in Pharmaceutical Sciences* 4 (2009) 105–112.
- [27] V. Lobo, A. Patil, A. Phatak, N. Chandra, Free radicals, antioxidants and functional foods: impact on human health, *Pharmacogn. Rev.* 4 (2010) 118–126.
- [28] B. Mahdi-Pour, S.L. Jothy, L.Y. Latha, Y. Chen, S. Sasidharan, Antioxidant activity of methanol extracts of different parts of *Lantana camara*, *Asian Pacific Journal of Tropical Biomedicine* 2 (2012) 960–965.
- [29] C.V. Jayachandran Nair, S. Ahamad, W. Khan, V. Anjum, R. Mathur, Development and validation of high-performance thin-layer chromatography method for simultaneous determination of polyphenolic compounds in medicinal plants, *Pharmacogn. Res.* 9 (2017) S67–S73.
- [30] M. Attimarov, K.K.M. Ahmed, B.E. Aldhubaib, S. Harsha, High-performance thin layer chromatography: a powerful analytical technique in pharmaceutical drug discovery, *Pharmaceutical Methods* 2 (2011) 71–75.
- [31] C.A. Simões-Pires, B. Hmicha, A. Marston, K. Hostettmann, A TLC bioautographic method for the detection of alpha- and beta-glucosidase inhibitors in plant extracts, *Phytochem. Anal.* 20 (2009) 511–515.
- [32] E. Azadniya, G.E. Morlock, Automated piezoelectric spraying of biological and enzymatic assays for effect-directed analysis of planar chromatograms, *J. Chromatogr. A* 1602 (2019) 458–466.
- [33] M. Jamshidi-Aidji, J. Macho, M.B. Mueller, G.E. Morlock, Effect-directed profiling of aqueous, fermented plant preparations via high-performance thin-layer chromatography combined with *in situ* assays and high-resolution mass spectrometry, *J. Liq. Chromatogr. Relat. Technol.* 42 (2019) 266–273.
- [34] M. Jamshidi-Aidji, G.E. Morlock, Fast equivalence estimation of unknown enzyme inhibitors *in situ* the effect-directed fingerprint, shown for *Bacillus* lipopeptide extracts, *Anal. Chem.* 90 (2018) 14260–14268.
- [35] S. Krüger, L. Hüskens, R. Fornasari, I. Scainelli, G.E. Morlock, Effect-directed fingerprints of 77 botanical extracts via a generic high-performance thin-layer chromatography method combined with assays and mass spectrometry, *J. Chromatogr. A* 1529 (2017) 93–106.
- [36] M.M. Rahman, M.N. Haque, S. Hosen, J. Akhter, U.S.B. Kamal, E.N. Jahan, A.S.M. S. Hossain, M.N. Uddin, M.B. Islam, M.R. Islam, A.H.M.K. Alam, A. Mosaddik, Comparative evaluation of antimicrobial activity of different parts of *Abelmoschus moschatus* against multi-resistant pathogens, *Int. J. Pharmaceut. Sci. Res.* 8 (2017) 1874–1880.
- [37] <https://case.edu/artscli/chem/faculty/salomon/Mechanisms.htm>; last access April 1st, 2020.
- [38] R.L. Jarret, M.L. Wang, I.J. Levy, Seed oil and fatty acid content in okra (*Abelmoschus esculentus*) and related species, *J. Agric. Food Chem.* 59 (2011) 4019–4024.